ACCELERATION COMPENSATED LOW LEVEL PRESSURE TRANSDUCER

by Samuel Lederman and Marian Visich, Jr.

Prepared under Grant No. NsG-409 *by*
POLYTECHNIC INSTITUTE OF BROOKLYN
Farmingdale, N.Y.
for

NATIONAL AERONAUTICS AND SPACE ADMINISTRATION • WASHINGTON, D. C. • AUGUST 1965

NASA CR-286

ACCELERATION COMPENSATED LOW LEVEL PRESSURE TRANSDUCER

By Samuel Lederman and Marian Visich, Jr.

Prepared under Grant No. NsG-409 by
POLYTECHNIC INSTITUTE OF BROOKLYN
Farmingdale, N.Y.

for

NATIONAL AERONAUTICS AND SPACE ADMINISTRATION

For sale by the Clearinghouse for Federal Scientific and Technical Information
Springfield, Virginia 22151 – Price $1.00

ACCELERATION COMPENSATED LOW LEVEL PRESSURE TRANSDUCER

By Samuel Lederman and Marian Visich, Jr.

Polytechnic Institute of Brooklyn
Farmingdale, New York

SUMMARY

The design and development of a miniature high sensitivity acceleration compensated crystal pressure transducer is described. It is shown that the transducer has the necessary characteristics in terms of response, sensitivity and linearity for application in low density shock tunnels and shock tubes. The pressure range can easily be varied over a wide range without affecting the resolution capability referred to the full scale of a given transducer.

INTRODUCTION

One of the most important parameters to be measured in an aerodynamic simulation facility is pressure. In principle pressure can be measured by a variety of methods. For example, pressure can be related to the displacement of a liquid column or diaphragm, to a change in an electric field (capacitive), to a change in magnetic field (reluctance), to charge generation (piezoelectric), to heat conduction or to ionization. In addition,pressure can be measured by means of mechanical methods such as Bourdon tube pressure gauges and strain gauges. The pressure level to be measured and the required response time would determine which of the aforementioned methods would be used.

For measurements in shock tubes and shock tunnels, the pressure range encountered is from a fraction of a millimeter of mercury to hundreds of atmospheres and running times ranging from microseconds to several milliseconds. As a result,the response time of the pressure measuring equipment must be on the order of microseconds. Since the tubing for a pressure tap on a model to a transducer and cavity must be as small as possible to minimize the response time, this puts a severe restriction on the size of the transducer. A further restriction on the size of the transducer to be used in a shock tube or shock tunnel facility is the fact that a model of limited size may require as many as 30 pressure transducers and heat transfer gauges to be installed internally. Another requirement for a pressure transducer for shock tunnel applications is that it be insensitive to vibration and temperature.

During an experimental program on the properties of the plasma sheath around hypersonic reentry bodies conducted in the hypersonic shock tunnel of the Polytechnic Institute of Brooklyn, a pressure transducer with the following specifications was required: a) small size, b) fast response, c) high sensitivity, d) pressure range from 5×10^{-6} atm. to 1 atm. and e) acceleration and temperature compensated. Commercially available transducers could not satisfy these requirements and a program was initiated to develop a pressure transducer for the experimental program on plasma sheaths. In this report the design and development of a crystal transducer which satisfies the aforementioned requirements is described.

SYMBOLS

τ	Poissons ratio
u	coefficient of viscosity
c_e	static capacity of the transducer crystal
c_{m_1}	compliance of crystal
c_{m_2}	compliance of diaphragm
c_{m_t}	total compliance of the transducer
d	diameter of tube
E	elastic modulus
f_r	resonance frequency
F	force
ℓ	length
ℓ_e	equivalent length
m	mass
N	open circuit voltage as a function of applied force
P	pressure
Q	charge
R	diaphragm radius
t	time
t_1	thickness of the crystal
t_2	" " " diaphragm
T	temperature
V	total volume of cavity and connection tubing
w	width of the crystal
y	beam deflection

TRANSDUCER DESIGN

The aim of this program was the development of a pressure transducer, which would be simple to construct and which would possess the following characteristics:

Diameter	0.5" max
Height	0.2"max
Resolution	0.001 psi
Pressure range up to	0.5 psi
Overload	15. psi
Linearity	2 %
Sensitivity	100 pcb/psi
Rise time	10μ sec
Acceleration Sensitivity	$5X10^{-4}$ psi/g

Since the pressure transducer was to be used in a shock tunnel with its inherent short running times it was decided to concentrate only on a crystal type transducer. Many crystal transducer designs have been reported in the literature. (Refs. 1,2,3,4). Most of the designs reported use the crystal element in compression or tension to achieve the desired signal output for a given pressure input. Due to the increased sensitivity of the crystal subjected to bending in terms of charge generation, several transducer configurations were evaluated using the crystal as a beam. Figs. 1 and 2 present schematic diagrams of two of the configurations studied. In Fig. 1, the crystals are stretched across the entire diameter of the transducer body and are clamped at the two ends. In Fig. 2, an arrangement is shown in which the crystals are used as cantilever beams (i.e. the crystals are clamped at one end). The transducer arrangements shown in Figs. 1 and 2 will hereafter be referred to as transducer type A and type B, respectively. Photographs of the assembled transducers and their components shown schematically in Figs. 1 and 2 are shown in Figs. 3 and 4, respectively. Mylar and a copper nickel alloy material were evaluated as diaphragm materials.

Two crystals are used in the transducer; one crystal is used as the transducer element and the second crystal, connected electrically in series opposition, serves as the acceleration and temperature compensating element. The force acting on the diaphragm is transmitted to the crystal corresponding to the transducer element, by a force transmitting pedestal and is separated from the acceleration compensating element by a metallic ring which serves as the common electrode. The ring is insulated from the body of the transducer by plexiglass inserts and contact between the ring and the crystal is established by a retaining threaded ring. This technique of mounting avoids the necessity of soldering electrical leads to the metalized surface of the crystal with the inherent difficulties, inaccuracies and damaging effects on the crystal due to the applied local heating required for soldering. The diaphragm, with the attached force transmitting pedestal, is then placed in position and retained by either a threaded or press fitted end cap. In the transducer design shown in Fig. 1, the crystals are mounted one above the other and are clamped along its perimeter, while in transducer design shown in Fig. 2 the crystals are mounted at diametrically opposite ends of the transducer and thus act individually as cantilever beams.

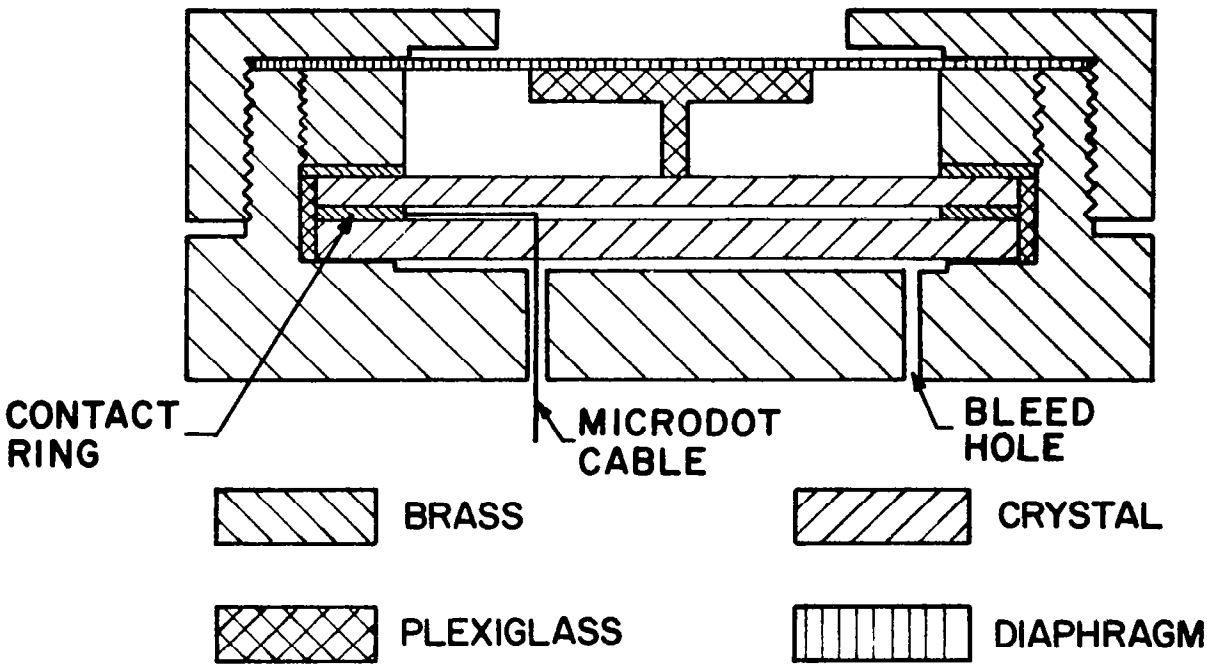

FIG. I. SCHEMATIC DIAGRAM OF A TYPE A TRANSDUCER

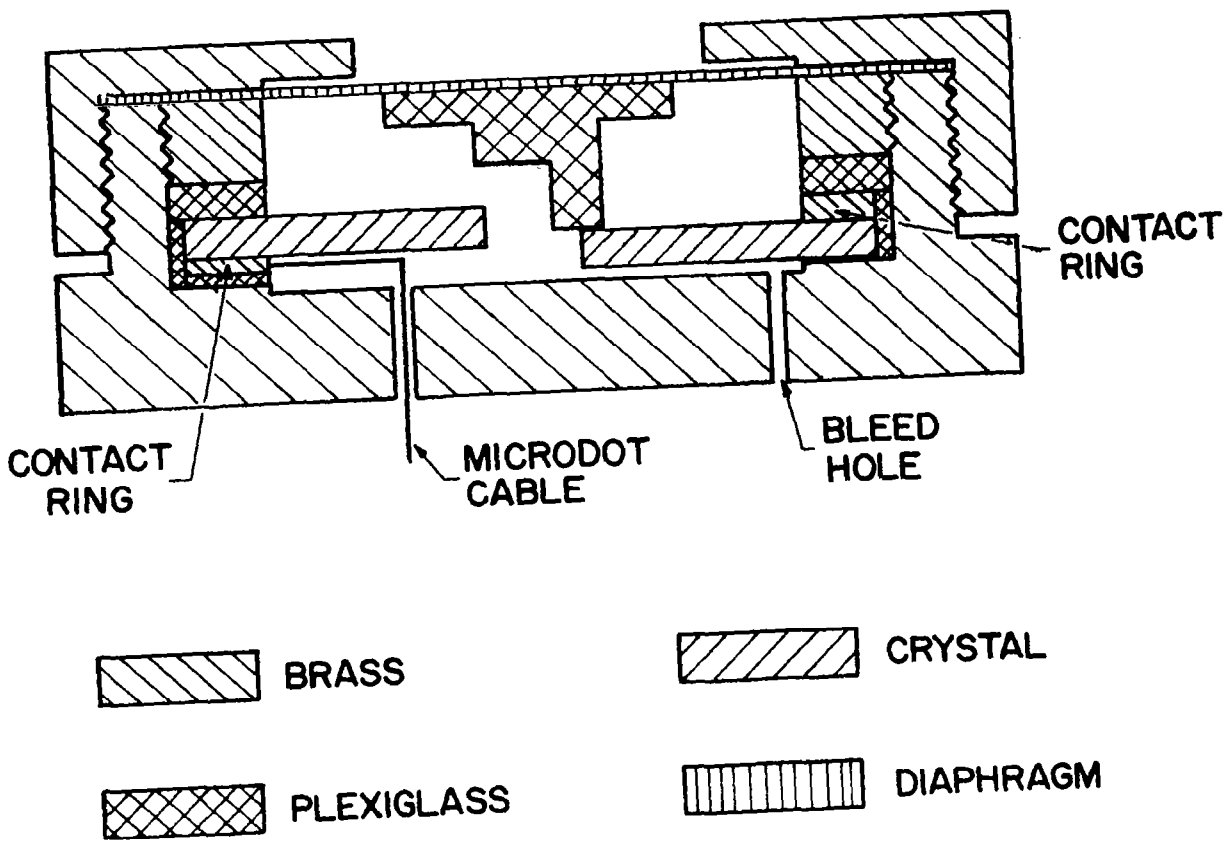

FIG. 2. SCHEMATIC DIAGRAM OF A TYPE B TRANSDUCER

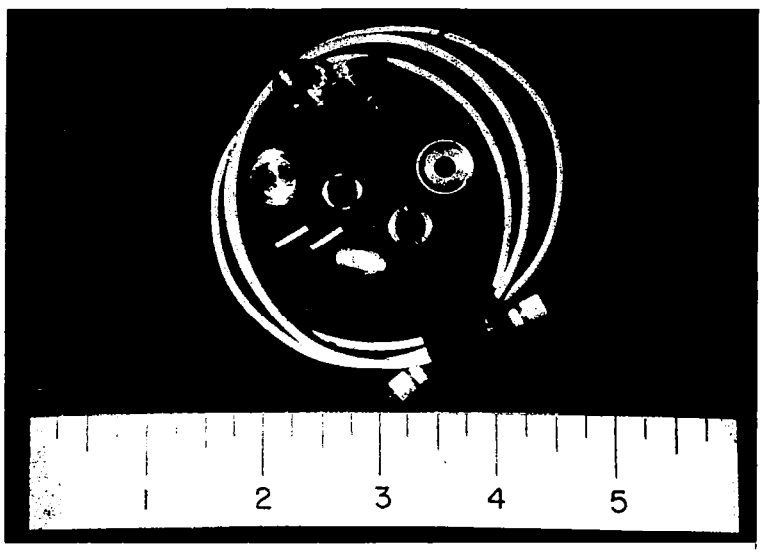

FIG. 3. PHOTOGRAPH OF THE TYPE A TRANSDUCER AND ITS COMPONENTS.

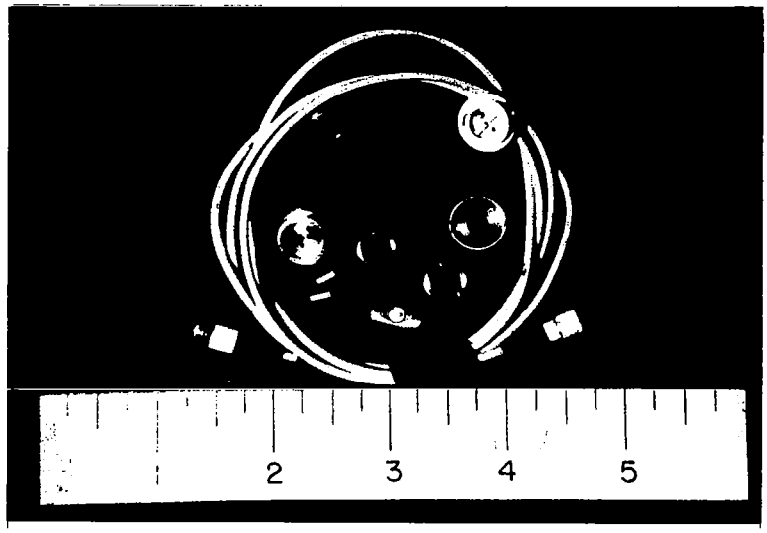

FIG. 4. PHOTOGRAPH OF THE TYPE B TRANSDUCER AND ITS COMPONENTS.

CALIBRATION OF THE TRANSDUCER

The transducers were calibrated using a semi-static method and a dynamic method. The physical arrangement of the equipment used for the semi-static calibration is shown schematically in Fig. 5. It consists of a tank with a volume of 2000 cm^3 connected to a cavity with a volume of approximately 1 cm^3 by a quarter turn quick opening valve. The transducer to be calibrated was mounted at the end of the cavity. In calibrating the transducer the tank was pressurized with the valve between the tank and the cavity closed to a given pressure level as measured by an inclined water manometer or baratron pressure gauge. The valve was quickly opened resulting in a pressure step to the transducer. The output of the transducer was amplified by a Kistler charge amplifier and monitored on an oscilloscope. The transducer was calibrated using this technique in the pressure range of 0.5 mm Hg. to 10 mm. Hg. At pressures above 5 mm. Hg. the calibrations were reproducible. At lower pressure levels, the semi-static technique resulted in excessive scatter of the data points. At 0.5 mm. of Hg. the scatter resulted in a maximum deviation of $\pm$ 50 % from the mean value.

In order to overcome the limitations of the semi-static method in the low pressure regime a calibration shock tube was constructed. A schematic diagram of the shock tube is shown in Fig. 6. For the calibration pressure range of interest behind the incident shock, an atmospheric pressure driver was found to be satisfactory. As a result, the room in which the shock tube was located acted as the shock tube driver, thereby increasing the possible running time of the test. The driven tube consisted of a 3-inch inside diameter tube 30 feet in length. The downstream end of the driven tube has 15 ports located 1-1/2 inches apart for mounting the transducers. The incident shock Mach number was determined using a time interval counter triggered by two pressure gauges located in the test region a known distance apart. With the initial pressure in the driven tube accurately determined, the pressure behind the incident shock wave can be obtained. By varying the initial pressure in the driven tube, the pressure behind the incident shock can be varied over a wide range. The outputs of the transducers were amplified by Kistler charge amplifiers and recorded on oscilloscopes.

DISCUSSION OF RESULTS

Several transducers of each design were fabricated and tested. Typical calibration curves for the two types of transducers using a 0.001 inch thick, mylar diaphragm are shown in Fig. 7 using the semi-static calibration technique. As can be seen from the calibration curves in this Figure the transducer type B is more sensitive than the transducer type A. It is worth noting at this point that both types of transducers exhibit a linear response. The deviation from linearity is better than the desired 2 %. Furthermore, as can be seen from these typical calibration curves, the sensitivity in the worst case exceeds the required sensitivity by a factor of 5. In both cases the resonant frequency of the transducer is greater than 400 kc, sufficient for a rise time on the order of 10 microseconds. Several transducers were tested in the PIB shock tunnel and it was found that the diaphragms were damaged after several tests due to impinging microscopic particles. These particles were more than likely formed during the breaking of the metallic diaphragm separating the combustion driver from the driven tube.

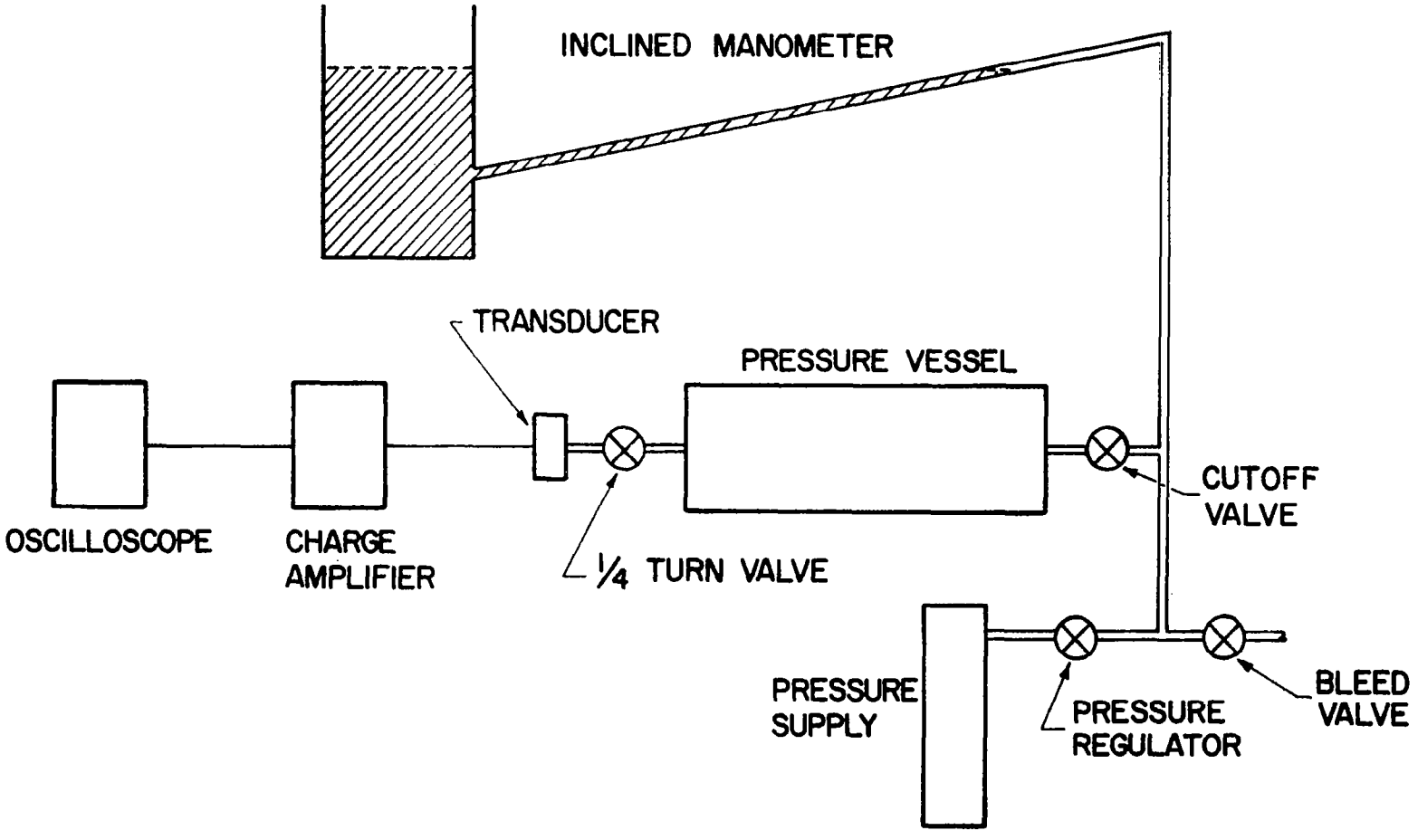

FIGURE 5. SEMI-STATIC CALIBRATION STAND.

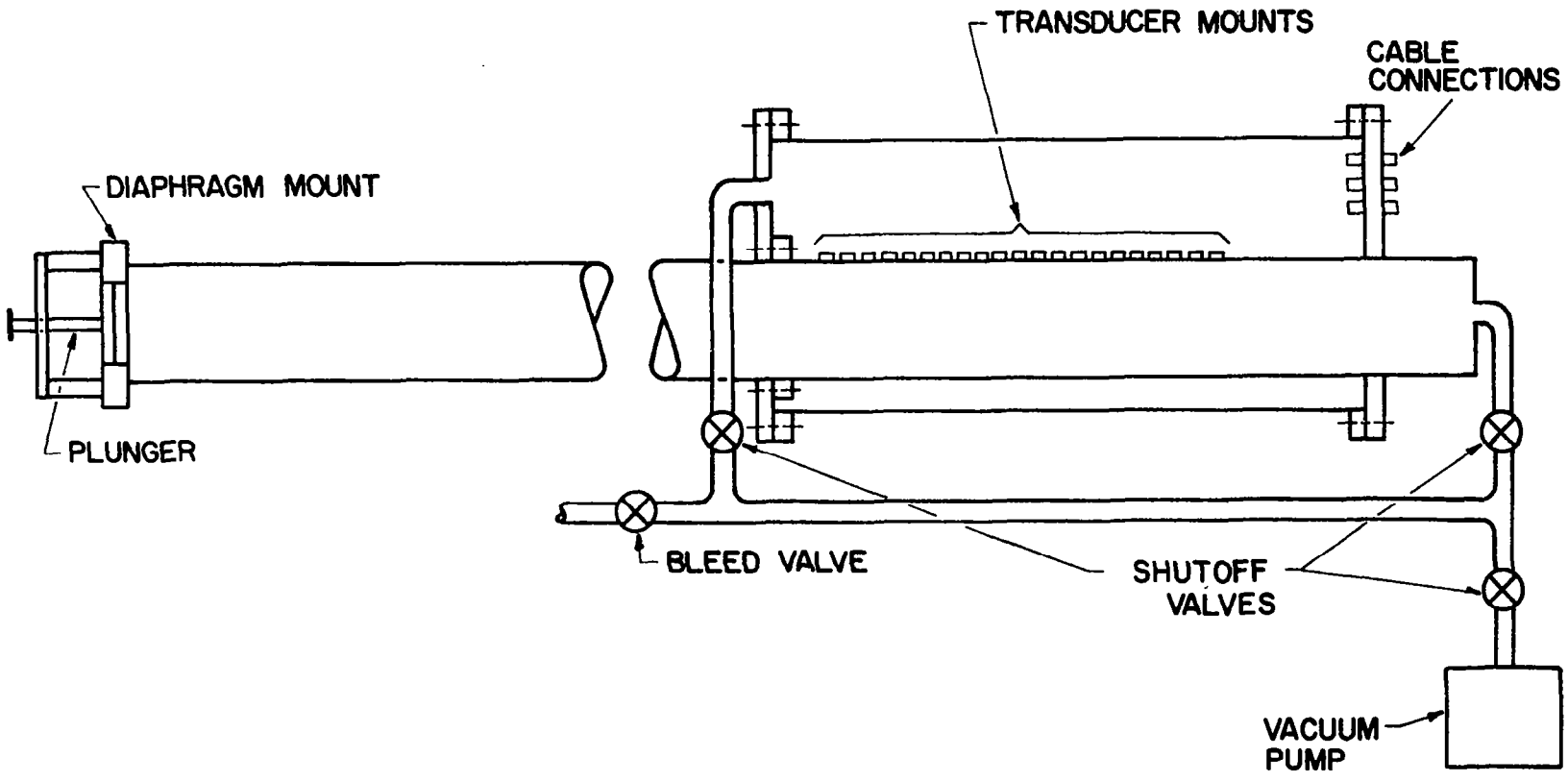

FIGURE 6. SCHEMATIC DIAGRAM OF THE CALIBRATION SHOCK TUBE.

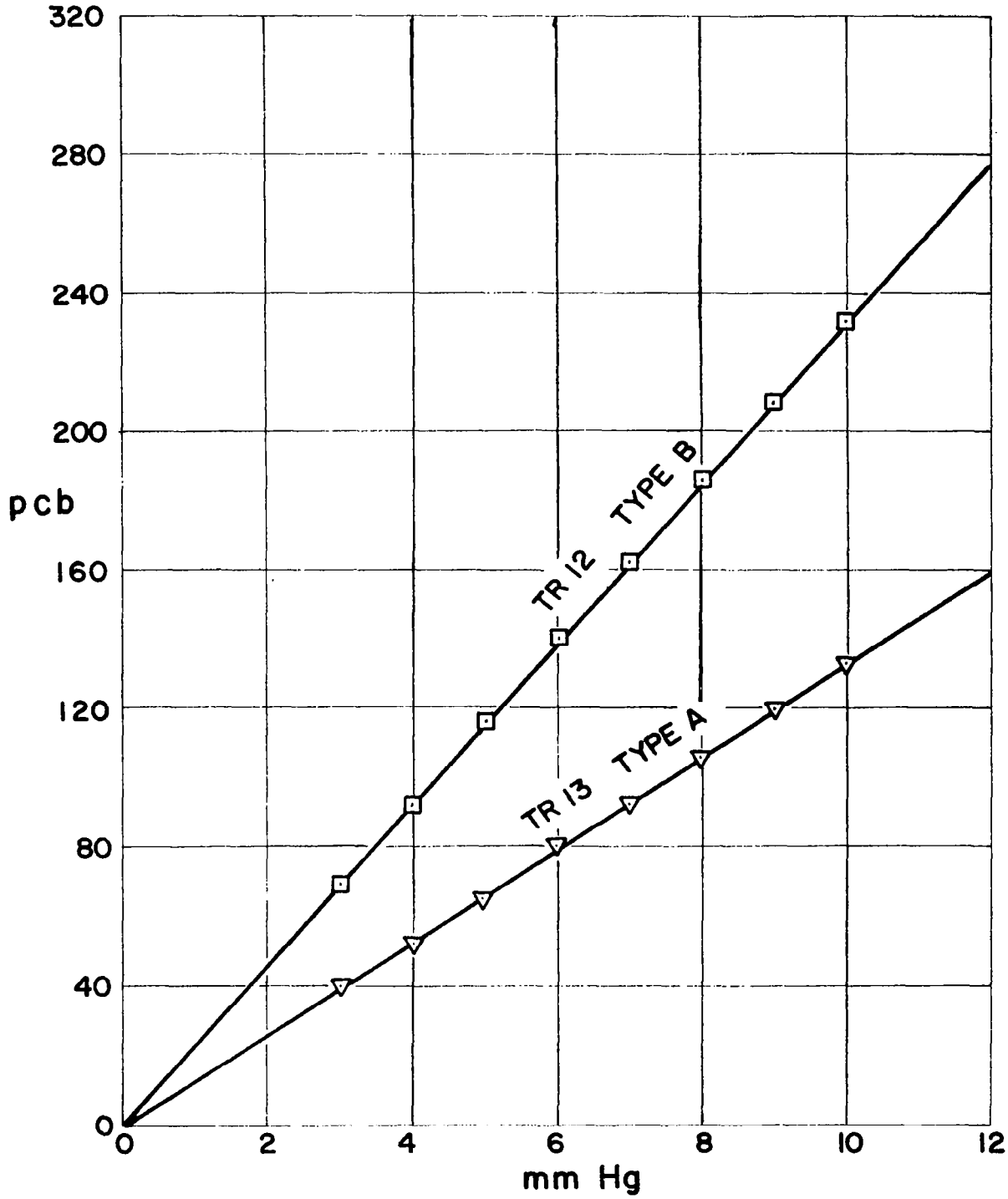

FIGURE 7. TYPICAL CALIBRATION CURVES FOR THE TWO TYPES OF TRANSDUCERS WITH MYLAR DIAPHRAGMS.

In order to increase the lifetime of the transducer the mylar diaphragm was replaced by a copper - nickel alloy diaphragm with a thickness of 0.0005 inch. Several transducers were calibrated using the metallic diaphragm and a typical calibration curve of the transducer type B is shown in Fig. 8. Also shown in this Figure is the corresponding calibration curve from Fig. 7 using a mylar diaphragm. Comparison of the calibration curves shown in Fig. 8 indicates that the sensitivity of the transducer with the metallic diaphragm is approximately 20 % higher than the same transducer with a mylar diaphragm.

Typical oscilloscope traces of the pressure transducer output obtained using the shock tube calibration method are shown in Fig. 9. These recordings show that the sensitivity of the individual transducers are slightly different. As shown in Appendix I, the sensitivity of the transducer is influenced by the thickness of the diaphragm, the unsupported length of the crystal, the dimensions of the crystal and the pedestal mount. These parameters can vary from transducer to transducer resulting in different sensitivities. The relatively slow response time of the transducers is due to the filter located in the circuit which had a time constant of approximately 10 μ seconds. The response of a transducer with and without a filter is shown in Fig. 10. The response time of the transducer without the filter is a function of the transducer configuration, and the orifice, tubing and cavity ahead of the transducer diaphragm (Appendix II). From the results shown in Fig. 10 it can be concluded that the response time of the transducer is below 10 μ seconds.

To determine the temperature characteristics of the transducer, calibration tests were made at several ambient temperature levels, in the range from 50°F. to 90°F. It was found that the transducer calibration did not change in that temperature interval. It was noticed, however, that when the ambient temperature changed the transducer output signal exhibited a slow drift until the transducer temperature reached a new equilibrium value. The transducer signal output due to this slow drift is equivalent to a pressure signal of less than 0.05 mm Hg/°F sec. Since the running time of the shock tunnel or shock tube is at most of the order of several milliseconds, the error in pressure measurement is negligible under the most adverse conditions. No extensive quantitative tests on the acceleration compensation properties of the transducer were conducted, due to the lack of the necessary equipment. However, some semiquantitative tests were made. Two transducers, one with the other without the acceleration compensating crystal, were mounted on a metal cantilever beam. The beam instrumented with strain gauges was subjected to vibration. The output of both transducers and the strain gauge bridge on the beam were observed on an oscilloscope. It was found that the transducer without the acceleration compensating crystals showed large signals, whereas the compensated transduced signals were considerably smaller. An approximate evaluation of the data indicated that the acceleration compensated transducer had a sensitivity of less than 5×10^{-4} psi/g. It was noticed however that the acceleration compensation is more effective for acceleration acting parallel than for acceleration acting normal to the diaphragm of the transducer. In the case of the acceleration acting parallel to the diaphragm, no signal could be observed on the oscilloscope.

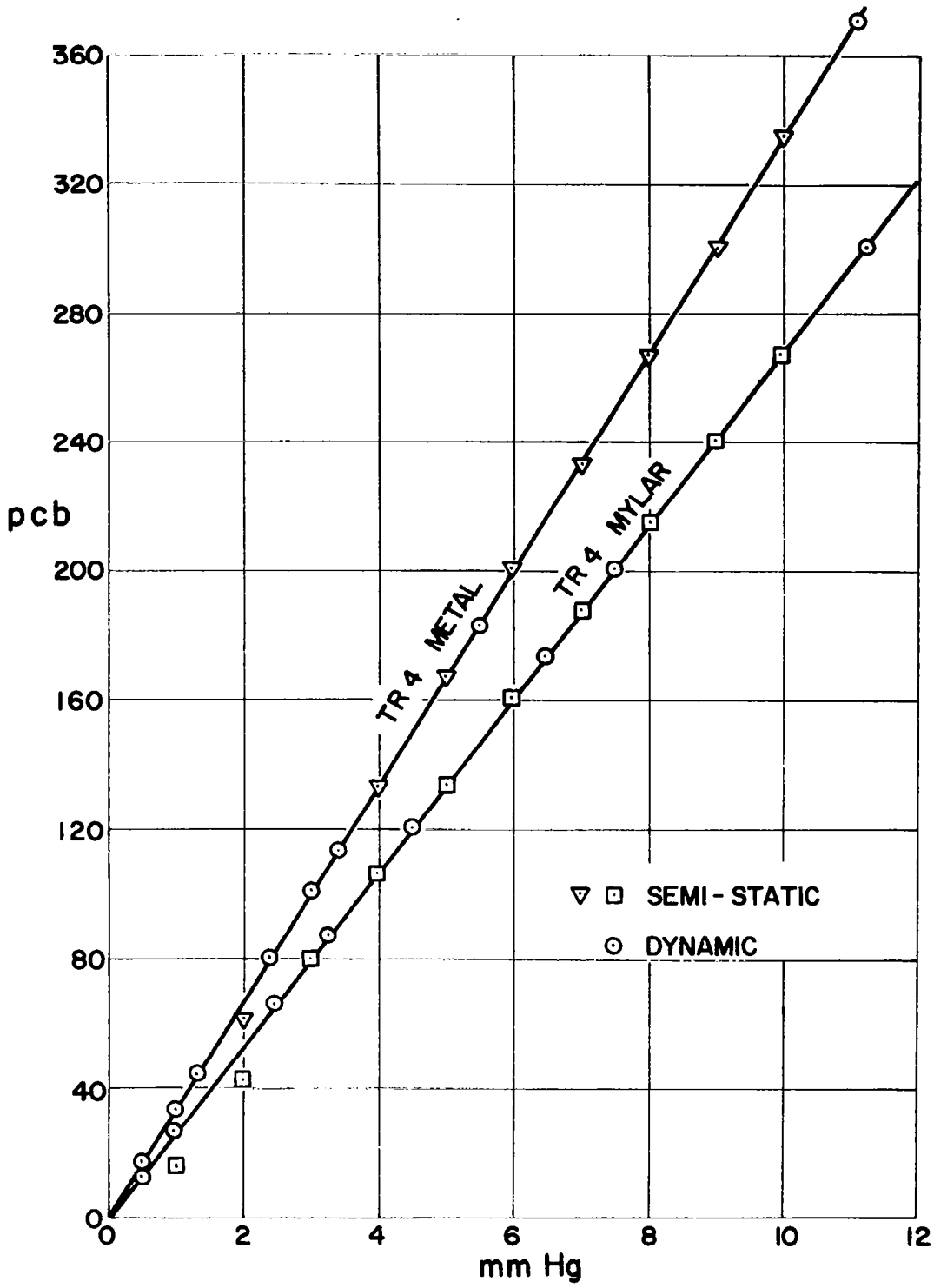

FIGURE 8. CALIBRATION CURVES OF THE TYPE B TRANSDUCER WITH 0.0005 METAL AND 0.001 MYLAR DIAPHRAGM.

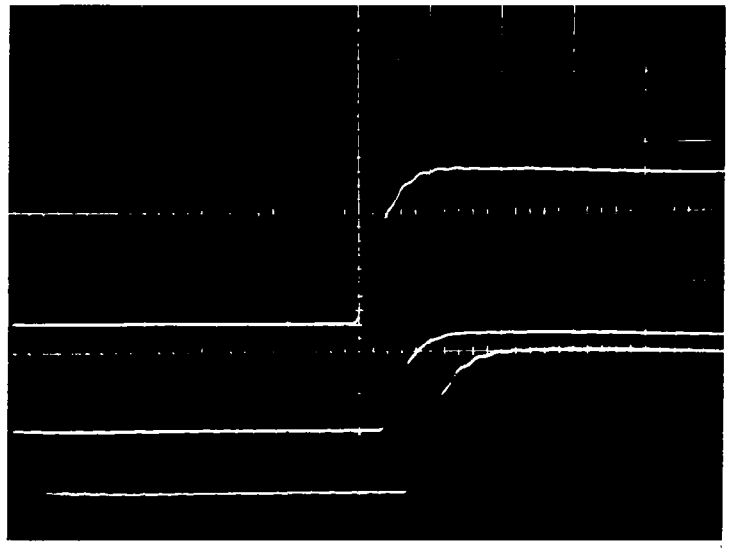

→ t

time scale 1 cm = 50μsec
vertical scale 1 cm = 100 mv

FIGURE 9. TYPICAL TRANSDUCER RESPONSE.

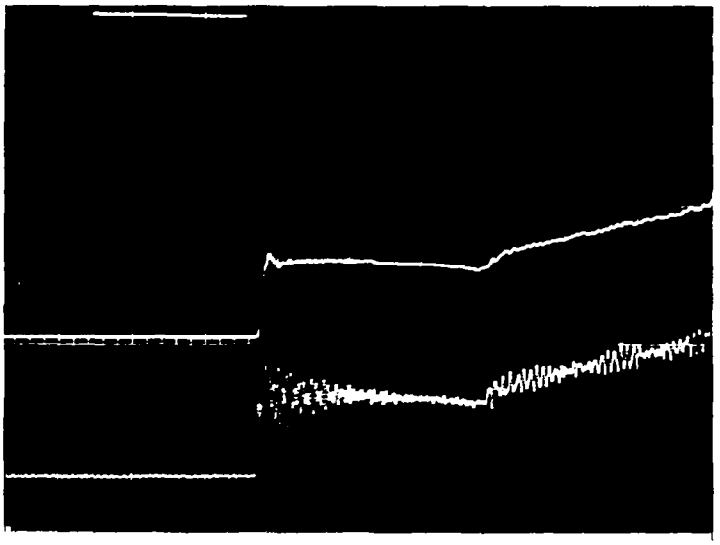

t

time scale 1 cm = 1 msec
vertical scale 1 cm = 100 mv

FIGURE 10. TRANSDUCER RESPONSE WITH AND WITHOUT A FILTER.

CONCLUDING REMARKS

Two types of miniature, high sensitivity, acceleration compensated, fast response crystal pressure transducers were developed, fabricated and tested. Both types of transducers were shown to possess the necessary characteristics for application in low density shock tunnels. It was also shown that the pressure range of the transducers can be readily changed. Evaluation of a number of transducers of the same kind indicated a certain degree of variations of the sensitivities. This variation in sensitivity could be related to the precision of fabrication. It is felt that more accurate tolerances and closer control of the fabricating procedures would result in a better agreement in the sensitivities of the individual transducers.

APPENDIX I

SENSITIVITY OF THE TRANSDUCER

An order of magnitude calculation of the output of the transducer can be obtained by means of the equivalent electromechanical circuit shown in Fig. 11a. In terms of the transducer crystal dimensions shown in Fig. 11b, the constants are given by:

$$C_e = \text{static capacity of the transducer crystal} = 325\ \frac{\ell w}{2\ t_c}\ (\mu\mu F) \tag{1}$$

N = open circuit voltage as a function of applied force

$$= .5\ \frac{\ell}{w t_1^3} \quad \text{(volts/Newton)} \tag{2}$$

Cm_1 = compliance i.e., ratio of deflection to applied force

$$= 2.8 \times 10^{-9}\ \frac{\ell^3}{w t_1^3} \quad * \text{ (meters/Newton)} \tag{3}$$

$$f_r = \text{resonant frequency of crystal} = 16\ \frac{t_1}{\ell^2} \quad \text{(kc)} \tag{4}$$

In terms of these constants the charge generated is given by:

$$Q = N C_e F = \frac{N C_e Y}{N^2 C_e + Cm_1} \sim \frac{N C_e Y}{Cm_1} \quad \text{(p c b)} \tag{5}$$

where

$$y = Cm_1 F$$

and F is the applied force in Newtons. Since the force corresponding to the applied pressure is not exerted directly on the crystal but through the intermediary diaphragm, the compliance Cm_1 of the crystal is modified by the compliance of the diaphragm. The compliance of the diaphragm is given by:

$$Cm_2 = \frac{3(1 - \sigma^2) R^2}{16 E t_2^3 \pi} \tag{6}$$

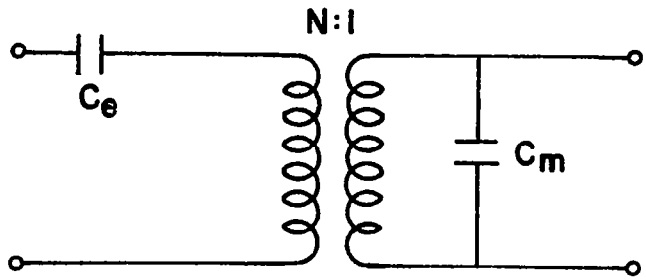

a) EQUIVALENT CIRCUIT

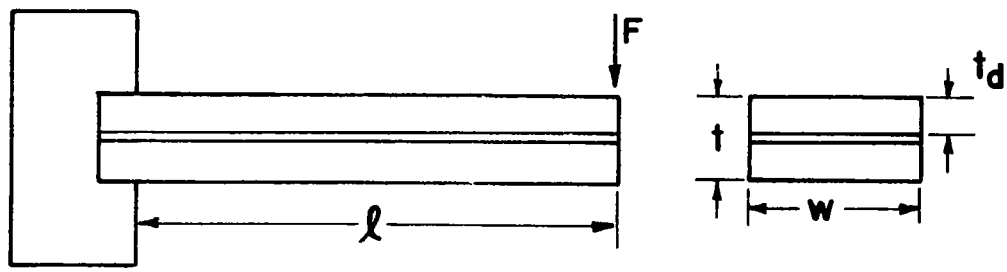

b) CANTILEVER SUSPENSION

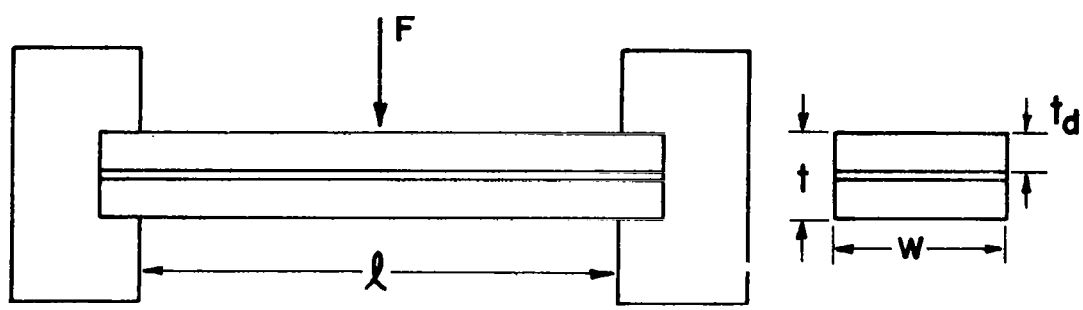

c) BEAM SUSPENSION

FIGURE 11. SUSPENSION TYPES AND EQUIVALENT CIRCUIT OF THE CRYSTAL.

where:

σ = Poissons ratio

R = diaphragm radius

t_2 = diaphragm thickness

E = elastic modulus of the diaphragm material

The total compliance of the system is therefore:

$$Cm_t = \frac{Cm_1 \quad Cm_2}{Cm_1 + Cm_2} \tag{7}$$

and the charge generated becomes:

$$Q = \frac{N C_e C_{mt} F}{Cm_1} \tag{8}$$

In terms of the applied pressure the charge generated is given by:

$$Q = \frac{N C_e Cm_t \pi R^2 P}{Cm_1} \tag{9}$$

It is evident from Eqs. (6), (7) and (9) that by changing the diaphragm thickness, the transducer sensitivity can be varied over a very wide range. In the case of the crystal beam clamped at both ends as shown in Fig. 11c, the equivalent electromechanical constants are given by:

$$C_e = 325 \frac{\ell w}{2 t_p} \quad (\mu\mu F) \tag{10}$$

$$N = 0.125 \frac{\ell}{w t_1} \text{ (Volts/Newton)} \tag{11}$$

$$Cm_1 = 0.175 \times 10^{-0} \frac{\ell^3}{w t_1^3} \text{ (meters/Newton)} \tag{12}$$

$$f_r = 45 \frac{t_1}{\ell^2} (Kc) \tag{13}$$

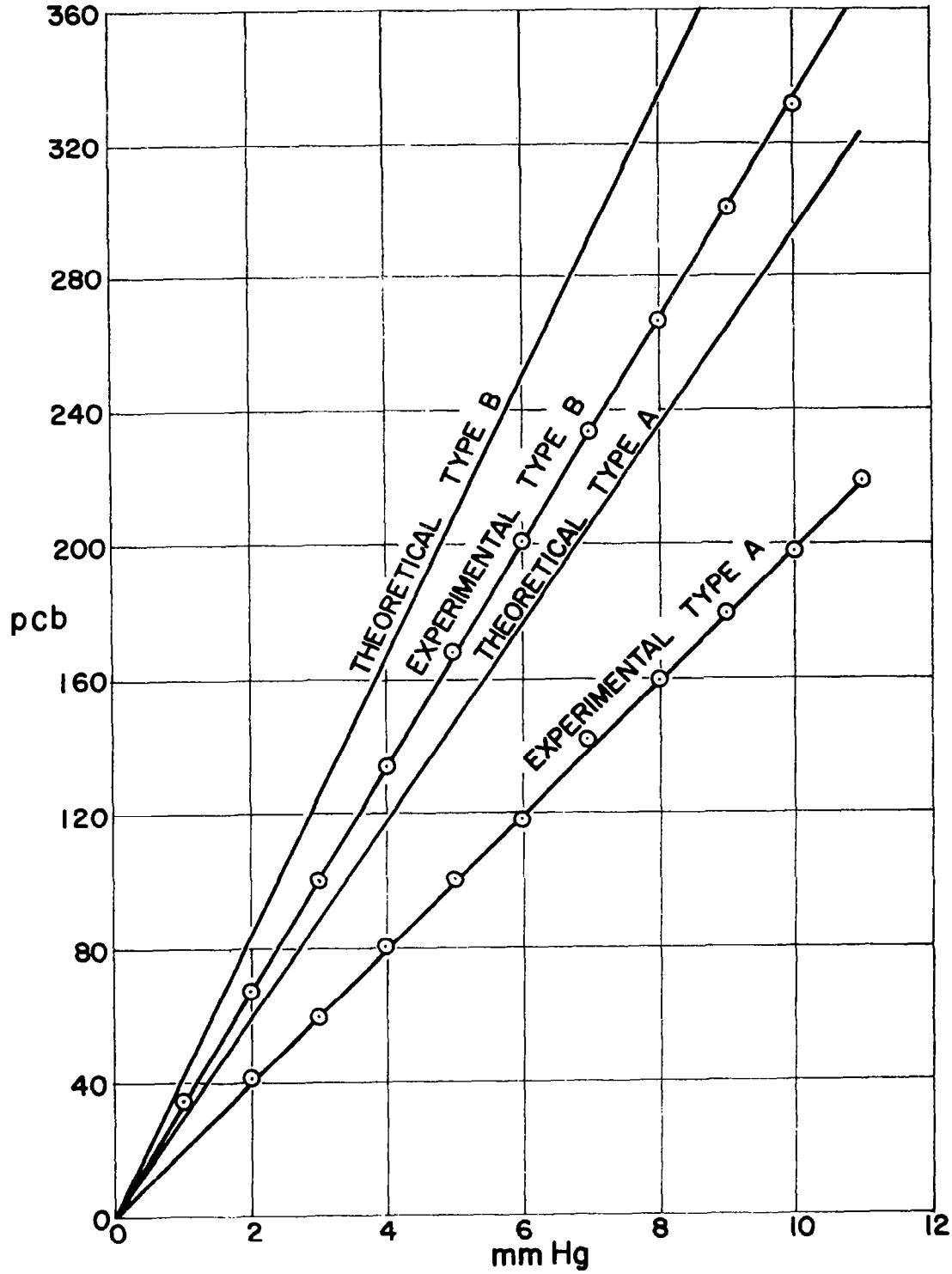

FIGURE 12. COMPARISON OF THE THEORETICAL AND EXPERIMENTAL OUTPUTS OF TWO TYPICAL TRANSDUCERS.

As in the case of the cantilever beam, the charge generated can be calculated in terms of these constants using Eqs. (5), (6), (7), (8) and (9).

The charge output obtained using Eq. (9) corresponds to the charge developed on the crystal. To measure the charge one can use a ballistic galvanometer, or connect the transducer to a charge amplifier and measure the voltage output as a function of charge. In the latter case one must take into account the cable capacity between the transducer and amplifier. A comparison of the theoretical output of a typical transducer and the experimental output as obtained using the charge amplifier is shown in Fig. 12. In the theoretical calculation the applied force to the crystal is assumed to be ideally applied at the end of the crystal in the case of the cantilever type transducer, and at a point in the center in the case of the crystal beam clamped at both ends, while in actuality the pedestal through which the force is applied has a finite dimension. As a result, the theoretical values shown in Fig. 12 are greater than the experimental values.

APPENDIX II

PRESSURE TIME LAG IN A CAVITY AND CONNECTING TUBES *

The configuration of the orifice, connecting tube and cavity of a pressure measuring system is shown in Fig. 13. The total volume of the tube orifice and cavity is denoted as a single volume V.

The rate of flow in a tube of circular cross section can be related to the pressure differential across the ends of the tube by means of the following equation:

$$\frac{dm}{dt} = \frac{\pi d^4}{256 \mu \ell_e RT} (P^2 - P_1^2) \tag{14}$$

where:

m = mass of air in the pressure measuring system (slug)

d = diameter of connecting tube(ft)

ℓ_e = equivalent length of tube orifice and cavity (ft)

P = pressure at any instant at the diaphragm of the transducer (lb/ft^2)

P_1 = pressure at the orifice (lb/ft^2)

R = universal gas constant

T = temperature (^oR)

μ = coefficient of viscosity (slug/ft sec)

If it is assumed that the process is isothermal, the mass flow rate is given by:

$$RT \frac{dm}{dt} = -P \frac{dv}{dt} - V \frac{dP}{dt} \tag{15}$$

---

* Refs.5, 6, 7.

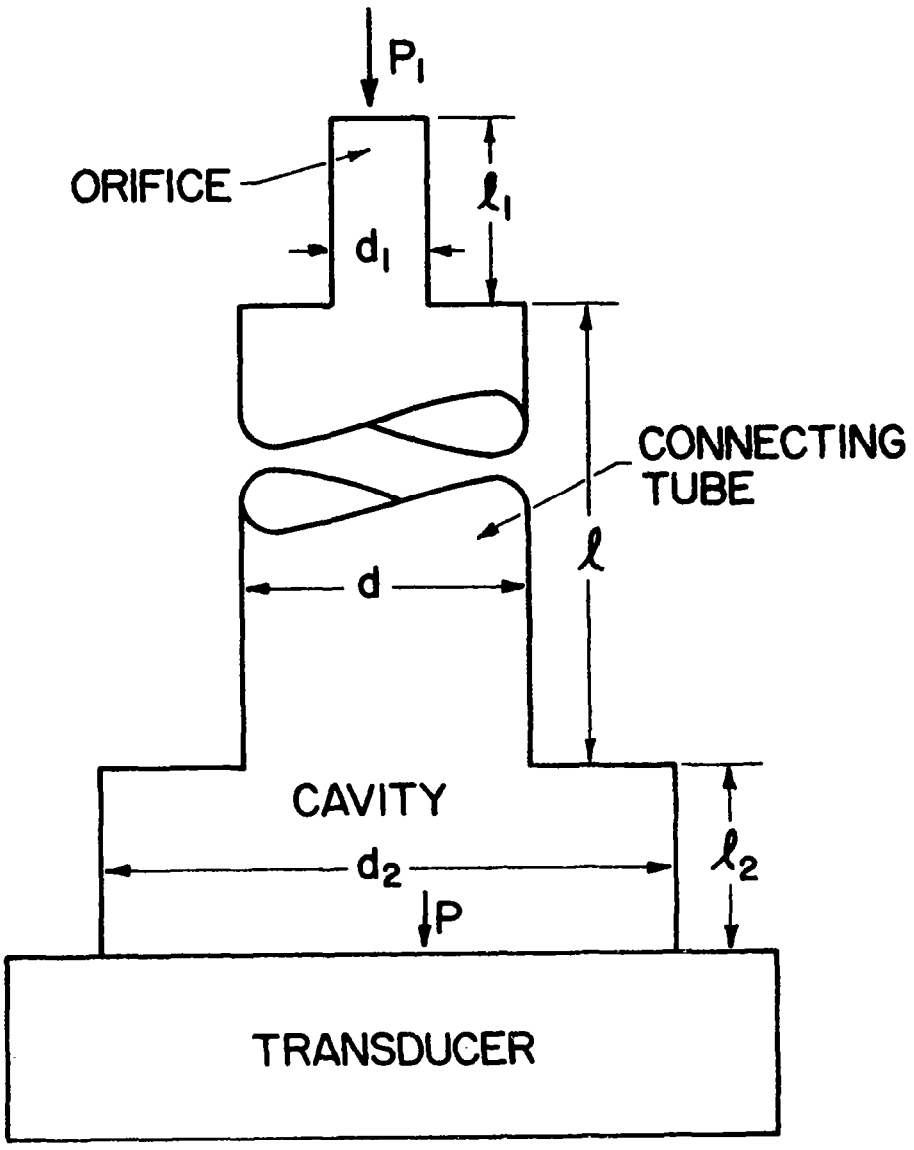

FIGURE 13. SCHEMATIC DIAGRAM OF A PRESSURE MEASURING SYSTEM.

Since the change in the volume of the system due to the deflection of the diaphragm is negligible Eq. (15) reduces to:

$$RT \frac{dm}{dt} = -V \frac{dP}{dt} \tag{16}$$

substituting Eq. (16) into (14) one obtains:

$$\frac{V}{RT} \frac{dP}{dt} = \frac{\pi d^4}{256 \mu \ell_e RT} (P^2 - P_1^2) \tag{17}$$

Integrating Eq. (17) one gets:

$$t + C = \frac{128 \mu \ell e V}{\pi d^4 P_1} \ell n \frac{P + P_1}{P - P_1} \tag{18}$$

Since at $t = 0$ $P = P_o$, the initial pressure at the diaphragm, Eq. (18) reduces therefore to:

$$t = \frac{128 \mu 1e V}{\pi d^4 P_1} \ell n \frac{(P + P_1)(P_o - P_1)}{(P - P_1)(P_o + P_1)} \text{ sec.} \tag{19}$$

Eq. (19) permits one to calculate the time necessary for the system to reach equilibrium within a predetermined error if a step pressure P_1 is applied at the orifice of the system.

The equivalent length of an orifice connecting tube and cavity of a pressure measuring system, based on a common diameter d, can be determined by finding the equivalent length of each and adding the resulting lengths.

Consider the diameter of an orifice and cavity to be d_1 and d_2 respectively, and their corresponding lengths ℓ_1 and ℓ_2. It follows from Eq. (19) that the equivalent length of the system is

$$\ell e = \ell + \ell_1 \left(\frac{d}{d_1}\right)^4 + \ell_2 \left(\frac{d}{d_2}\right)^4 \tag{20}$$

where ℓ and d are the length and diameter of the connecting tube, respectively.

REFERENCES

1. Hopkins, H. B., Scheuing, R. A. and Leng, J., Investigation of Pressure Distribution Over Planar, Twisted and Cambered Wings in a Hypersonic Shock Tunnel. Grumman Aircraft Engineering Corporation, Report No. ASD-TDR-62-171, May 1962.

2. Martin, J. F., Duryea, G. R., Stevenson, L. M., Instrumentation for Force and Pressure Measurements in a Hypersonic Shock Tunnel. Cornell Aeronautical Laboratory, Report No. 113, January 1962.

3. Levine, D., Acceleration-Compensating Pressure Transducers for Surface-Pressure Measurements. NAVORD Report No. 6834, January 1961.

4. Kaplan, K., Wilton, C. W., and Willoughby, A. B., Development of a Miniature Dynamic Pressure Gauge. Broadview Research Corporation, January 1961.

5. Jones, H. B., Transient Pressure Measuring Methods. Princeton University, Report No. 595a, NASA Contract No. NASr-36, January 1962.

6. Sinclair, A. R. and Robins, W., A Method for the Determination of the Time Lag in Pressure Measuring Systems. NACA TN 2793, September 1952.

7. Davis, W. T., Lag in Pressure Systems at Extremely Low Pressures. NACA TN 4334, September 1958.